Elastic Scattering and Cross Sections in Antiproton-Proton Interactions at 3.3 and 3.7 BeV/c*

T. FERBEL, A. FIRESTONE, J. SANDWEISS,† AND H. D. TAFT
Yale University, New Haven, Connecticut

M. GAILLOUD‡ AND T. W. MORRIS
Brookhaven National Laboratory, Upton, New York

AND

A. H. BACHMAN, P. BAUMEL, AND R. M. LEA
The City College, New York, New York

(Received 26 October 1964)

The elastic, the pion-production, and the multipion-annihilation cross sections for antiproton-proton interactions at 3.28 and 3.66 BeV/c incident antiproton momenta have been measured. A comparison of the elastic interactions at 3.28 BeV/c with a purely-absorbing disc optical model gave a best value for the radius of interaction of 1.3 F. The real part of the forward scattering amplitude has been found to be less than 20% of the imaginary part. A study of the asymmetries in double elastic scatters yielded a value for a polarizing power of the hydrogen consistent with zero when averaged over production angles.

INTRODUCTION

THIS paper is the first of a series reporting the results of a collaboration between the City College of New York, Brookhaven National Laboratory, and Yale University in an investigation of high-energy $\bar{p}-p$ interactions begun in the fall of 1961 at the Brookhaven AGS. An electrostatically separated beam and the 20-in. liquid-hydrogen bubble chamber were used to obtain approximately 50 000 pictures at 3.28 BeV/c, and 250 000 pictures at 3.66 BeV/c antiproton momentum.[1] There were approximately 15 antiprotons per pulse entering the bubble chamber.

A wide variety of reactions has been investigated; specifically elastic scattering, pion production without annihilation, annihilations with the production of pions, and the associated production of hyperons and kaons. This first paper will be concerned primarily with the elastic interactions and with summary of the major cross sections at the two energies.

THE SEPARATED BEAM

A high-energy electrostatically separated beam was designed and constructed at the Brookhaven AGS during 1960 and 1961. It has been used in conjunction with the 20-in. liquid-hydrogen bubble chamber in the study of pion-proton and kaon-proton as well as antiproton-proton interactions.[2] Figure 1 shows the experimental arrangement at the AGS. The beam consists of four main sections; the transport section, two similar velocity separator stages, and a beam shaping section. The transport section produces an image at slit 2 of the target in the F-10 straight section. The two velocity separation stages use standard electrostatic separators (crossed electric and magnetic fields) to effect mass separation; precise momentum definition is achieved through the large bending magnet located between the two separation stages. The shaping section defocuses the beam vertically and focuses it horizontally in order to properly fill the bubble chamber. Detailed descriptions of the beam are available in the literature,[2] and a complete study is also available.[3] The antiproton beam entering the bubble chamber had a momentum dispersion, $\Delta p/p$, of $\pm 2\%$, and an antiproton purity of approximately 95% as determined by counter techniques. A full description of the design and performance of the 20-in. liquid-hydrogen bubble chamber is also available in the literature.[4]

In order to gain a better understanding of the nature of the beam contamination, a scan was performed for all δ rays (knock-on electrons) with energies greater than 8 MeV. At an incident particle momentum of 3–4 BeV/c, the maximum energy that can be transferred to an electron at rest is a strong function of the mass of the beam particle. The maximum energy which can be delivered by an antiproton of 3.28 BeV/c momentum to an electron at rest is 12.3 MeV, while a π^-, μ^-, or e^-

* Research carried out under the auspices of the U. S. Atomic Energy Commission and the National Science Foundation.

† Alfred P. Sloan Foundation Fellow.

‡ Present address, Ecole Polytechnique, Lausanne, Switzerland.

[1] In the literature we have, in the past, referred to these beam momenta as 3.25 BeV/c and 3.69 BeV/c. Recent studies indicate the best values to be 3.28 BeV/c and 3.66 BeV/c, each with an uncertainty in the average value of 0.02 BeV/c and with a spread of $\pm 2\%$.

[2] C. Baltay, H. N. Brown, J. Sandweiss, J. R. Sanford, M. S. Webster, and S. S. Yamamoto, in *Proceedings of the 1962 Conference on Instrumentation for High-Energy Physics at CERN*, edited by F. S. M. Farley and M. E. Meyer (North-Holland Publishing Company, Amsterdam, 1963,) p. 37; J. Leitner, G. Monetti, and N. P. Samios, *ibid.* p. 42; C. Baltay, J. Sandweiss J. Sanford, H. Brown, M. Webster, and S. Yamamoto, Nucl. Instr. Methods 20, 37 (1963).

[3] C. Baltay, Doctoral dissertation, Yale University, 1963 (unpublished).

[4] D. C. Rahm, *Proceedings of the International Conference on High-Energy Accelerators and Instruments, CERN*, (CERN Scientific Information Service, Geneva, 1959). R. I. Louttit, Proceedings of the International Conference on Instrumentation for High Energy Physics, Berkeley, 1960 (unpublished).

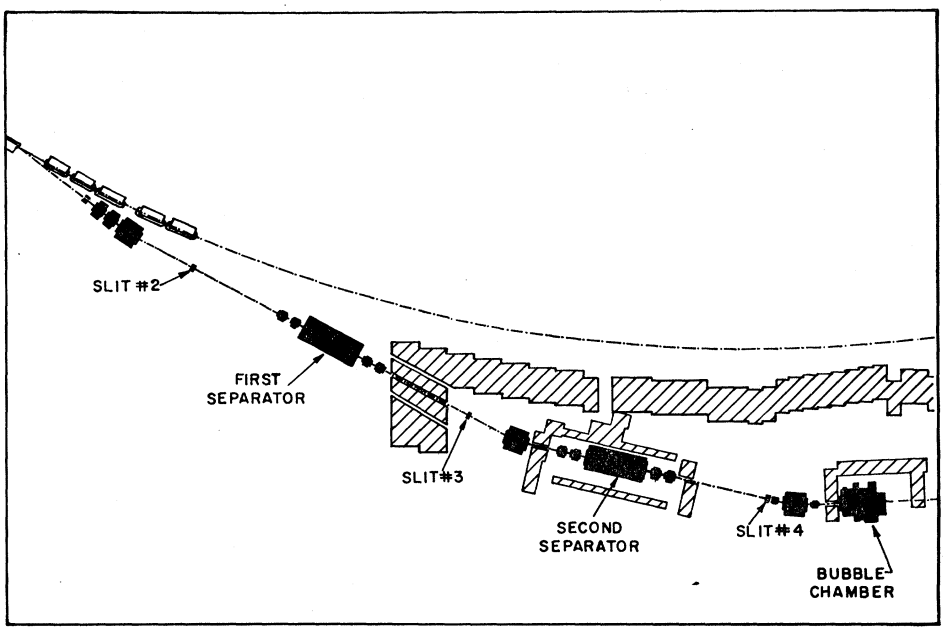

FIG. 1. Layout of the separated beam on the floor of the AGS.

of the same momentum can deliver up to 475, 754, or 3280 MeV, respectively. At a momentum of 3.66 BeV/c, $\bar{p}$, π^-, μ^-, and e^- can transfer up to 15.6, 591, 937, and 3660 MeV, respectively. Figure 2 shows the experimental δ ray energy spectra and the expected energy distribution of δ rays for various degrees of antiproton purity.[5] The curves for both momenta have been normalized to the experimental points at 9 MeV.

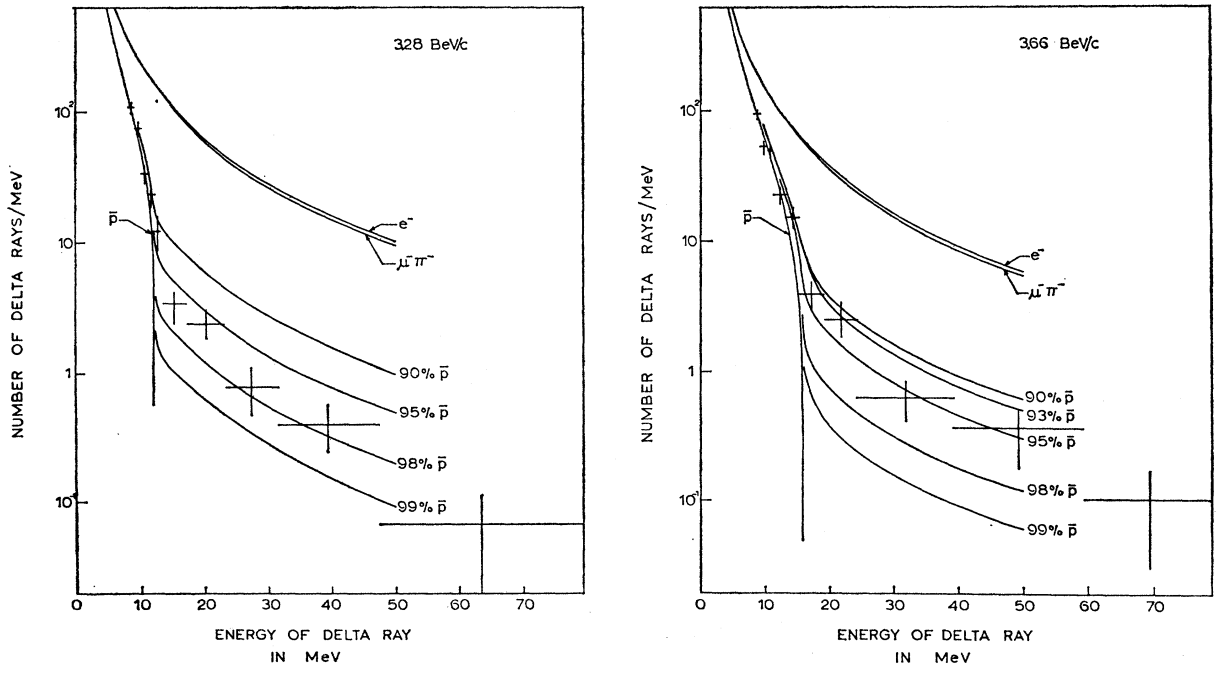

FIG. 2. Delta ray spectra in the 3.28-BeV/c and 3.66-BeV/c antiproton beams. The solid curves show the expected energy distribution for delta rays for the indicated degrees of antiproton purity.

[5] The comparison spectra are from a calculation by Bhabha of the collision probability of particles of spin 0 and spin $\frac{1}{2}$ on electrons at rest. The spin dependence at 3–4 BeV/c beam momentum is negligible, and we have used the spin 0 calculation. For further details see B. Rossi, *High Energy Physics* (Prentice-Hall, Inc., Englewood Cliffs, New Jersey, 1952) and H. J. Bhabha, Proc. Roy. Soc. (London), **164**, 257 (1938).

At 3.28 BeV/c, the data are consistent with 97±1% antiproton purity, while at 3.66 BeV/c the beam is consistent with 94±1% antiproton purity. At 3.28 BeV/c, 54 δ rays had energies greater than 13 MeV. The beam tracks which caused these δ rays did not interact strongly in the path length remaining to them. On a basis of a π^- contamination one strong interaction was expected. The null result is consistent with a μ^- background. Similar considerations at 3.66 BeV/c indicated a 3% μ^- and a 3% π^- contamination.

CROSS SECTIONS

A total of 3000 two prongs, 8000 four prongs, 2000 six prongs, and 300 eight prongs were measured at 3.28 BeV/c and 3.66 BeV/c.[6] Table I summarizes the results of the major elastic and inelastic $\bar{p}-p$ cross sections at the two energies. Table II summarizes the cross sections for the major pion production and annihilation channels.

The cross sections in Tables I and II have been corrected for scanning losses and beam contamination. The beam path length has also been corrected for attenuation. At 3.28 BeV/c a correction of 3.7 mb was applied to the observed elastic cross section. This was done to correct for scanning losses in the small-angle elastic interactions (short recoils). The correction was based on the assumption that the shape of the optical-model prediction is correct for small angles (see next section). Although the elastic scattering at 3.66 BeV/c was not studied, it was assumed for cross-section calculations that the ratio of $\sigma_{\text{elastic}}/\sigma_{\text{2-prong}}$ is approximately the same as at 3.28 BeV/c.

A value of 0.0623±0.0006 g/ml was obtained for the density of the liquid hydrogen in the bubble chamber under operating conditions. This value was determined from a study of the range of μ^+ mesons produced when π^+ mesons stopped and decayed in the chamber.[7] The errors quoted in Table I and in Table II contain the estimated systematic as well as the statistical errors.

TABLE I. Major cross sections for $\bar{p}-p$.

Category	3.28 BeV/c σ(mb)	3.66 BeV/c σ(mb)
0 prongs	4.0 ±0.4	4.5 ±0.4
2 prongs	41.5 ±1.3	37.3 ±1.3
4 prongs	22.9 ±0.9	21.6 ±0.9
6 prongs	6.6 ±0.4	7.7 ±0.4
8 prongs	0.44±0.10	0.6 ±0.1
Total	75.4 ±2.0	71.7 ±2.0
Elastic	21.9 ±1.1	
Inelastic (all)	53.5 ±2.3	
Charge exchange ($\bar{p}p \to \bar{n}n$)[a]	$0.0_{-0.0}{}^{+1.3}$	
Pion production without annihilation[b]	19.2 ±2.0	
Annihilation into pions	30.9 ±3.0	
Annihilation into kaons and pions[c]	2.9 ±0.2	2.3 ±0.3
Hyperons[c]	0.44±0.05	0.71±0.08

[a] Obtained by subtraction of inferred pion production states and measured strange particle cross sections.
[b] Contains 6.3 mb correction for the inferred reactions $\bar{p}p \to \bar{n}n+\cdots$. See T. Ferbel, A. Firestone, J. Sandweiss, H. D. Taft, M. Gailloud, *et al.*, Phys. Rev. (to be published).
[c] N. Yeh, and C. Baltay (personal communication), see also Ref. 3.

[6] The topology of an n-prong final state consists of an incoming negative track which interacts in the chamber giving rise to n outgoing charged particles.

STUDY OF ELASTIC INTERACTIONS

Approximately 3000 two prongs at 3.28 BeV/c were measured and analyzed using the GUTS kinematic fitting program.[8] Figure 3 shows the χ^2 distribution for a sub sample of the events which were fitted to an elastic scattering interpretation. The smooth curve is the shape of the 4-constraint χ^2 distribution normalized to the 1135-event sample. A χ^2 scale factor[9] of 1.8 was used to give a reasonable fit to the data. This indicated that our assumed errors were on the average too small by about 35%. A large fraction (~30%) of the elastic events were originally classified as kinematically ambiguous events. These were the events which were consistent with at least one one-constraint (one missing neutral particle) annihilation interpretation in addition

TABLE II. Major pion production and annihilation channels for $\bar{p}-p$.

Category	3.28 BeV/c σ(mb)	3.66 BeV/c σ(mb)
Single pion production (All)[a]	8.6 ±1.5	
$\bar{p}p\pi^0$	2.3 ±0.5	
$\bar{n}p\pi^-$ and $n\bar{p}\pi^+$[b]	4.0 ±0.6	
$\bar{p}p\pi^+\pi^-$	3.43±0.23	3.67±0.30
$\bar{p}p\pi^+\pi^-\pi^0$	0.3 ±0.1	0.5 ±0.1
$\bar{p}n\pi^+\pi^+\pi^-$ and $p\bar{n}\pi^+\pi^-\pi^-$	0.3 ±0.1	0.4 ±0.1
$\bar{p}p\pi^+\pi^+\pi^-\pi^-$	≥0.01	
Annihilation into $\pi^+\pi^-$ or K^+K^-	<0.025	
$\pi^+\pi^-\pi^0$	0.7 ±0.4	
$2\pi^+2\pi^-$	0.76±0.08	
$2\pi^+2\pi^-\pi^0$	4.5 ±0.6	
$3\pi^+3\pi^-$	0.95±0.12	
$3\pi^+3\pi^-\pi^0$	2.90±0.25	
$4\pi^+4\pi^-$	0.10±0.03	
$4\pi^+4\pi^-\pi^0$	0.25±0.06	

[a] Contains estimated $\sigma(\bar{p}p \to \bar{n}n\pi^0) = 2.3$ mb.
[b] The cross section for $p\bar{p} \to n\bar{p}\pi^+$ was not measured directly as this state was found to be indistinguishable from the annihilation states. This cross section was assumed to be the same as $\sigma(\bar{p}p \to \bar{n}p\pi^-)$, which is required by CP invariance.

[7] M. Rich and R. Madey, University of California Radiation Laboratory Report UCRL 2301, 1954 (unpublished).
[8] J. P. Berge, F. T. Solmitz, H. Taft, Rev. Sci. Instr. **32**, 538 (1961).
[9] A. H. Rosenfeld and W. E. Humphrey, Ann. Rev. Nucl. Sci. **13**, (1963).

to the elastic interpretation. Most of the ambiguous events were resolved on the basis of ionization. The remaining events had coplanarity, χ^2, and missing mass distributions similar to those of the unambiguous elastic interactions.[10] On this basis, and because of the fact that it is much less likely that a one-constraint interaction will simulate an over-determined four-constraint interpretation, rather than the reverse, all the ambiguous events have been included with the elastic interactions.

A study of the expected bias in right-left as opposed to up-down scattering of the recoil proton in the elastic events indicated severe losses at small momentum transfers. Figure 4 shows the distribution in an angle ψ, the azimuth of the emerging proton using the beam track direction as the polar axis, as a function of the cosine of the center-of-mass scattering angle ($\cos\theta_{\text{c.m.}}$), where $\psi=0°$ is defined by a plane perpendicular to the camera axis. The distributions have been folded into one quadrant. At very small scattering angles ($\cos\theta\gtrsim 0.990$),

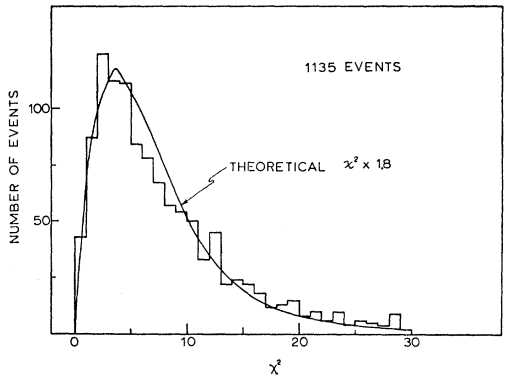

FIG. 3. χ^2 distribution of the elastic events at 3.28 BeV/c (4-constraint fit.)

the losses in the region $60°\leq\psi\leq 90°$ are almost complete, but for larger scattering angles ($\cos\theta_{\text{c.m.}}\lesssim 0.980$) the effect is not as strong. Since the losses were restricted almost entirely to regions where ψ was within 30° of the camera axis ($60°<\psi\leq 90°$), it was decided to include in our further studies of the elastic interactions only those events which had a ψ of the proton recoil within 60° of "flat" ($0°\leq\psi\leq 60°$).

The center-of-mass angular distribution of elastically scattered antiprotons at 3.28 BeV/c is shown in Fig. 5. The experimental data are compared with the shapes predicted by a simple absorbing-disc optical model for radii 1.2, 1.3, and 1.4 F.[11] The optical model for a purely

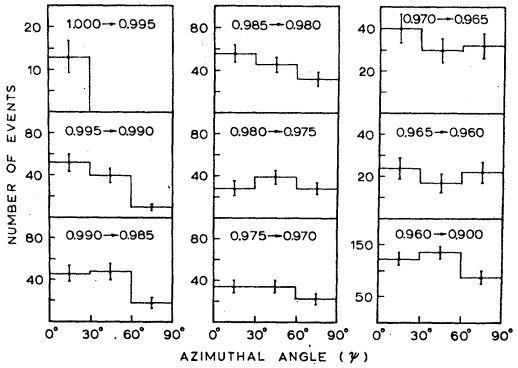

FIG. 4. Azimuthal distribution of the outgoing proton about the incoming antiproton direction as a function of the center-of-mass scattering angle of the antiproton. Events with $60°\leq\psi\leq 90°$ are in the biased region. The numbers in each box give the interval in $\cos\theta_{\text{c.m.}}$.

absorbing disc of radius R, without phase shift, gives

$$\frac{d\sigma_{\text{elastic}}}{d\Omega}=\frac{\sigma_{\text{elastic}}}{\pi}\left[\frac{J_1(kR\sin\theta)}{\sin\theta}\right]^2,$$

$$\sigma_{\text{elastic}}=\pi R^2|1-A|^2,$$

$$\sigma_{\text{inelastic}}=\pi R^2[1-|A|^2],$$

where J_1 is the first order Bessel function, k is the center-of-mass wave number, and A is the amplitude of the transmitted wave. The shape of the theoretical curve for $R=1.3$ F gives the best fit to the experimental

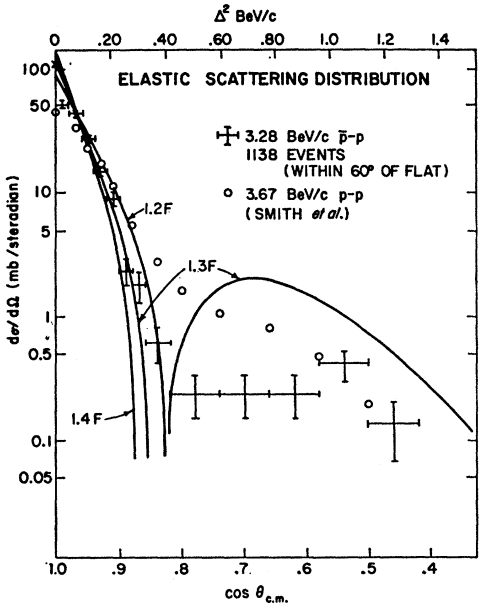

FIG. 5. Angular distribution of the antiproton in $\bar{p}-p$ elastic scattering events at 3.28 BeV/c incident momentum. The solid curves are predicted by a simple absorbing-disc optical model with radii 1.2, 1.3, and 1.4 F. The point at $\cos\theta_{\text{c.m.}}=1.0$ is obtained from the optical theorem. The open circles show the $p-p$ data at 3.67 BeV/c.

[10] T. Ferbel, Doctoral dissertation, Yale University, 1963 (unpublished).

[11] S. Fernbach, R. Serber, T. B. Taylor, Phys. Rev. **75**, 1352 (1949). B. Cork, W. A. Wenzel, and C. W. Causey, *ibid.* **107**, 859 (1957).

TABLE III. Optical-model parameters.

	$\bar{p}-p$ at 3.28 BeV/c	$p-p$ at[a] 3.04 BeV/c	$p-p$ at[b] 3.67 BeV/c
R	1.30±0.05 F	0.93 F	0.93 F
σ_{elastic}	21.9 ±1.1 mb	17±3 mb	15.3 ±0.8 mb
A	0.38±0.03	0.21	0.26
σ_{elastic} calculated	45.6 ±2.5 mb	26 mb	26.4 mb
σ_{elastic} observed	53.3 ±2.3 mb	26±3 mb	27.2 ±1.6 mb
opacity ($=\sigma_{\text{inel (obs)}}/\pi R^2$)	0.98±0.05	0.96	0.96±0.06

[a] Reference 12.
[b] Reference 13.

points at small angles. The low point in the first interval is not physical; it is caused by the lack of sensitivity of the bubble chamber to low-momentum recoils (small-angle losses). The forward scattering point ($\theta=0°$) in Fig. 5 was calculated by applying the optical theorem assuming that the forward scattering amplitude is purely imaginary. Table III summarizes the parameters for this absorbing disc model.

This simple optical model is adequate for angles for which $\cos\theta \gtrsim 0.85$. A check of the consistency of the model using the best fit radius and the experimental value of the elastic cross section reveals a poor agreement between the calculated and observed inelastic cross sections. A better fit to the elastic events for large angle scattering can be obtained through a more sophisticated model using a short-range phase shift and tapering of the edges of the absorbing disc.[11–13] In Fig. 5, for comparison, we have also included the proton distribution in $p-p$ scattering at 3.67 BeV/c. Both the $\bar{p}-p$ and $p-p$ scattering spectra are diffraction-like, but the sharper peaking and somewhat larger elastic cross sections for the $\bar{p}-p$ system reflect the larger $\bar{p}-p$ inelastic cross section resulting from the large annihilation channels which are available only to the $\bar{p}-p$ system. The inconsistency between the observed and calculated inelastic $\bar{p}-p$ cross sections indicates that this simple optical model is more appropriate to the pp than to the $\bar{p}p$ system.

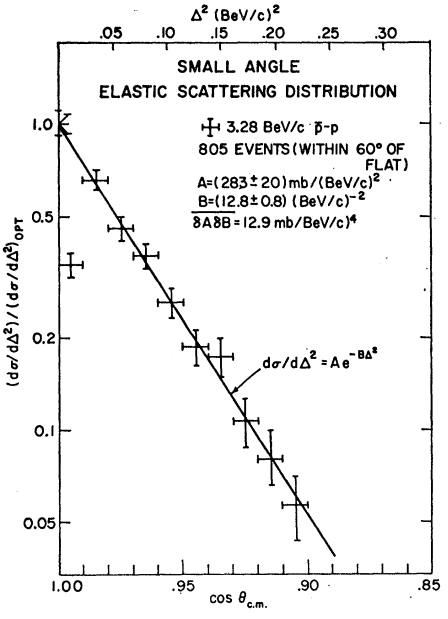

FIG. 6. Angular distribution of the antiproton in $\bar{p}-p$ elastic scattering for $\cos\theta_{\text{c.m.}}<0.85$. The solid curve is a linear least-squares fit (on the semilog scale) to the nine points with $\Delta^2<0.25$ (BeV/c)^2.

Figure 6 shows the elastic-scattering distribution at small angles. A least squares fit to a function of the form

$$d\sigma/d\Delta^2 = Ae^{-B\Delta^2},$$

where Δ^2 is the square of the four-momentum transfer to the proton, indicates that the real part of the forward scattering amplitude must be less than 20% of the imaginary part and is consistent with a purely imaginary forward scattering amplitude. These results are in agreement with the CERN data at similar energies.[14]

POLARIZATION STUDIES

A possible polarization of the antiprotons produced in the AGS target was investigated using the elastic interactions in the bubble chamber as analyzers. A distribution in the angle ϕ is expected to be of the form $I_0(\theta)(1+e_1\cos\phi)$, where ϕ is the angle between the normal to the production plane at the AGS and the normal to the elastic scattering plane in the bubble chamber, θ is the scattering angle of the antiproton in the elastic interaction, and $e_1(=P_1P_2)$ is the product of the polarizing power (P_1) of the AGS target with the analyzing power (P_2) of the proton target in the bubble chamber; both P_1 and P_2 being functions of the production (scattering) angles.

A sample of 525 elastic events at 3.28 BeV/c, with the scattering angle larger than 3° and with an average value of about 5° in the laboratory, gave a value of $e_1=0.029\pm0.062$, consistent with either P_1 or P_2 or both being zero. A similar procedure was followed in the analysis of double elastic scatters in the bubble chamber. It was assumed that the incoming antiproton beam was unpolarized and therefore a distribution in the angle ϕ, the angle between the normals to the two scattering planes for double scatter events (with both interactions occurring at the same scattering angle, θ) was again expected to be of the form $I_0(\theta)(1+e_2\cos\phi)$, where e_2 is now defined as P_2^2, the average of the square of the polarizing (analyzing) power of the hydrogen.

A total of 123 double elastic events at 3.28 and 3.66 BeV/c with both scattering angles between 2.5° and 9.0° in the laboratory and with an average value of 4.7°

[12] W. J. Fickinger, Doctoral dissertation, Yale University, 1961 (unpublished).
[13] G. A. Smith, H. Courant, E. C. Fowler, H. Kraybill, J. Sandweiss, and H. Taft, Phys. Rev. 123, 2160 (1961).
[14] O. Czyzewski, B. Escoulies, Y. Goldschmidt-Clermont, M. Guinea-Moorhead, T. Hofmokl, *Proceedings of the Sienna International Conference on Elementary Particles, 1963*, edited by G. Bernadini and G. P. Puppi (Societa Italiana Di Fisica, Bologna, 1963), Vol. I, p. 252.

gave a value for $e_2=P_2^2=0.081\pm0.127$, consistent with zero polarization. There is some depolarization of the antiprotons between the two elastic scatters due to the fact that the polarization vector precesses in the magnetic field of the bubble chamber. This was investigated and the effect of the precession was found to be on the average less than 2% of $\cos\phi$ and so was ignored. The distribution in the angle ϕ was consistent with isotropy, and the absence of any $\cos\phi$ dependence is consistent with a zero value for e_2. From our values of $e_1=P_1P_2$ and $e_2=P_2^2$, we obtain for the average $P_1^2=0.010\pm0.029$, consistent with zero beam polarization.

Our result of $e_2=P_2^2=0.081\pm0.127$ is in agreement with the results of Czyzewski *et al.*[14] at 3–4 BeV/c of $P^2=0.050\pm0.080$. These results should be compared with the data of Button *et al.*,[15] who obtained a value of $P^2=0.26\pm0.10$. at 1.6 BeV/c. As pointed out by Czyzewski *et al.*,[14] there is a decrease in the polarization with increasing bombarding energy, when the polarization is averaged over a wide range of scattering angles.

ACKNOWLEDGMENTS

We wish to acknowledge the many contributions by individuals of the AGS, BNL, and Yale bubble chamber staffs which made this work possible. We also wish to thank the computer center staffs at Yale, NYU, and BNL for their courtesy and assistance throughout this experiment. Mr. N. Yeh's contribution in the early stages of the analysis of the data is greatly appreciated.

[15] J. Button and B. Maglic, Phys. Rev. **127**, 1297 (1962).

PHYSICAL REVIEW VOLUME 137, NUMBER 5B 8 MARCH 1965

Unitary or Octal Symmetry?

G. Cocho*

Instituto de Fisica, Universidad de Mexico, Mexico City, Mexico

(Received 24 June 1964; revised manuscript received 7 October 1964)

Octal symmetry (R_8=group of rotations in eight dimensions) is applied to the strong interactions. If the existence of an octet m and a singlet λ of spinless mesons is assumed, a bootstrap mechanism allows the existence of 36 vector mesons with the coupling constants given by the R_9 group. Under $R_8\subset R_9$ the 36-plet of vector mesons splits in an octet v' [with η (780), K(730), π(560) as a possible identification] and a 28-plet v. From octal symmetry a multiplicative quantum number N (block parity) is obtained which forbids the decay $v'\to m+m$ and perhaps explains the small width of this octet. A reasonable mass formula allows us to predict the masses of the v,v' vector mesons and suitable candidates with the predicted masses are found. The partial widths for the $v\to m+m$ decays are consistent with the experimental data and in particular with $\Gamma_{K(1175)\to K\pi}$, $\Gamma_{\pi(1220)\to\pi\pi}$ being small.

I. INTRODUCTION

THE unitary symmetry octet model[1] has been applied recently with fair success in order to explain different features of the elementary particles.[2] The purpose of this work is to show that the experimental data are compatible (and in some cases show a better agreement) with the predictions of octal symmetry (R_8=group of rotations in eight dimensions).

Gürsey,[3] Ne'eman,[4] and Gourdin[5] have applied the R_8 group to the physics of the weak and strong interactions. In this paper, we will extend the physical applications, in order to include some of the newly found resonances and their properties—quantum numbers, decay widths, etc.

II. OCTAL SYMMETRY AND BLOCK PARITY

The dimensions of the representations of the R_8 algebra are: 1, 8^i, 28, 35^i, 56^i, etc., where the index $i=0, 1, 2$, labels three "analogous nonequivalent representations.[6] In particular, 8^0 is the vector representation and 8^1 [8^2] is the first [second] kind of semispinor representation.

For the decomposition of some of the direct products we have[6,7]:

$$8^i\otimes 8^i=1\oplus 28\oplus 35^i, \tag{1}$$

$$8^{(1,2)}\otimes 8^0=8^{(2,1)}\oplus 56^{(2,1)}, \tag{2}$$

$$8^1\otimes 8^2=8^0\oplus 56^0, \tag{3}$$

$$8^i\otimes 28=8^i\oplus 56^i\oplus 160^i. \tag{4}$$

* Technical Consultant to the Comisión Nacional de Energía Nuclear.

[1] M. Gell-Mann, Report CTSL-20, 1961 (unpublished); Phys. Rev. **125**, 1067 (1962); Y. Ne'eman, Nucl. Phys. **26**, 222 (1961).

[2] Y. Ne'eman, Conference on Symmetry Principles at High Energies, Coral Gables, Florida, 1964 (unpublished).

[3] F. Gürsey, Ann. Phys. (N.Y.) **12**, 91 (1961).

[4] Y. Ne'eman, Phys. Letters **4**, 81 (1963).

[5] M. Gourdin, Nuovo Cimento **30**, 587 (1963). This author discusses in an explicit way the algebra of $R_8\supset SU_3/Z_3$.

[6] E. Cartan, *Leçons sur la Théorie des Spineurs* (Herman et Cie., Paris, 1938).

[7] R. Brauer and H. Weyl, Am. J. Math. **57**, 425 (1935).